TWO-DIMENSIONAL POPULATION BALANCE MODELLING OF SEMI-BATCH ORGANIC SOLUTION CRYSTALLIZATION

Puel, F. and Févotte, G.

LAGEP, UMR CNRS 5007, Université Lyon 1, 43 bld. Du 11 novembre 1918. 69100 Villeurbanne. FRANCE

Abstract: A population balance model simulates the time variations of two characteristic sizes of hydroquinone particles during crystallization. The population balance equations combined with kinetic models and mass balance equations allowed the simulation of the crystallization of hydroquinone characterized by a rod-like habit. Semi continuous isothermal operations were performed at the lab-scale in the presence of various additive concentrations. Both the experimental supersaturation trajectory and the final bi-dimensional Crystals Size Distribution (CSD) were correctly predicted by the model. The simulated elongation factor characterizing the crystal shape was therefore in agreement with the experimental one. For secondary nucleation, indirect effects were assumed to occur and satisfactory predictions of the final number of fine particles were obtained. A major interest of the two-dimensional model lies in its ability to relate the time variations of the crystal habit : the particles lengthen in the first moments of their growth and then progressively get thicker until the end of the process.

Keywords: Modelling, Particulate Processing, Parameter Estimation, Chemical Industry, Partial Differential Equations, Batch Processes.

1. INTRODUCTION

In the field of industrial crystallization most authors have focused their efforts on modelling one characteristic parameter of the particles, generally a given equivalent size (Franck et al., 1988; David et al., 1991). Nevertheless, the usual one-dimensional approach does not suitably describe the evolution of a population of anisotropic crystals, which is the common case with organic products. This is why a two dimensional population balance approach was presented and solved numerically (Puel et al., 2003a), in order to simulate the time variations of two sizes of crystals. Actually, the industrial production of fine organics may lead to problems arising from the lack of mastery of the end-use properties of the crystals. These problems are due to the high sensitivity of the crystal habits to the effects of supersaturation, impurities and additives during the crystallization operation. It is therefore useful to analyse and predict the evolution of crystal habits during the process.

At the solid state, hydroquinone exhibits a rod like habit (see Fig.1), with three main dimensions: length L_1, width L_2 and height, assumed to be equal to the width. An elongation shape factor, F_1, is also defined as the length to width ratio. To take into account the two sizes and the shape of the crystals, two-dimensional population balance equations are required. Such modelling strategy will be applied to determine the kinetic parameters of the crystallization process.

Batch experiments have rich information contents and are therefore suitable for satisfactory parameter estimation of the nucleation and growth mechanisms. However the time variations of temperature require taking into account the temperature dependency of the kinetic parameters. Consequently, isothermal semi-batch operation appears as a good strategy to obtain a set of kinetic parameters since it allows distinguishing between the various phenomena occurring as a function of time. At the beginning, the process is dominated by primary nucleation, afterwards the crystal growth gets the upper hand,

and secondary nucleation takes a significant part in the size variations when the concentration of crystals is sufficient. The crystallization of hydroquinone was therefore experi-mentally carried out in a semi-batch isothermal well-mixed crystallizer. In addition to usual kinetic investigations, the effect of various concentrations of a tailor-made additive was also studied. The semi-batch crystallization of hydroquinone was then simulated using a bi-dimensional population balance approach.

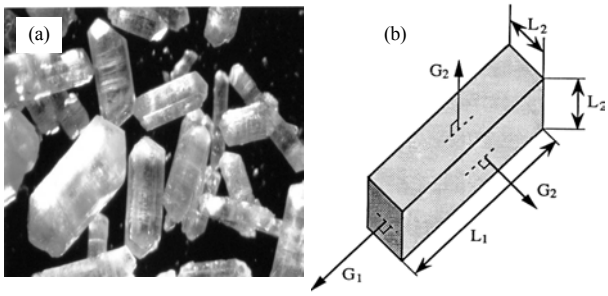

Fig. 1. (a) Photographic picture of typical crystals of hydroquinone and (b) bi-dimensional approxi-mation of the corresponding rod-like particles.

2. EXPERIMENTAL SETUP AND OPERATING CONDITIONS

2.1 Experimental setup

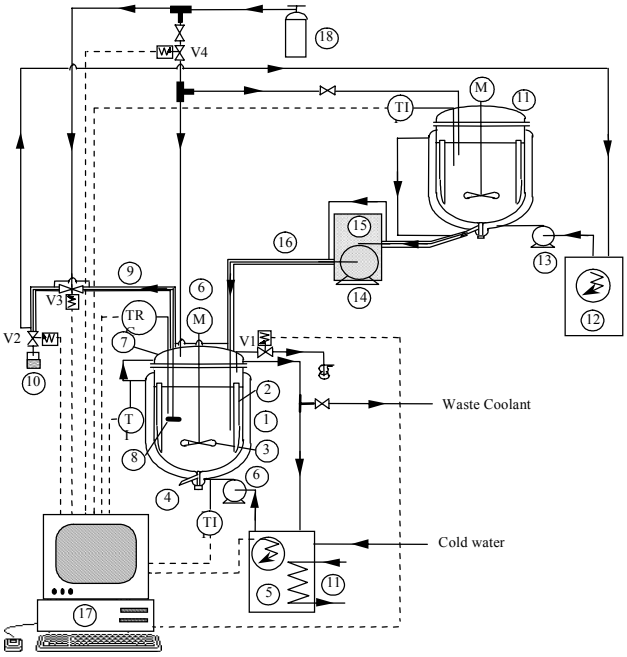

Fig. 2. Experimental apparatus

The experimental device is shown schematically in Fig. 2. The crystallizer (1) is a glass reactor equipped with four baffles (2) and a Mixell TT propeller (3). The suspension is withdrawn from the vessel using the bottom valve (4). A constant temperature is maintained in the crystallizer by using a thermostatic bath (5) and a circulating pump (6). The coolant goes through a glass jacket and a jacketed cover (7). Four electrovalves were sequentially manipulated to perform the withdrawal of solution samples through a filter (8). Samples were diluted for titration. The feed tank (11) was thermostated (12), the transfer of the hot undersaturated solution to the crystallizer was carried out using a peristaltic pump (14) and jacketed pipes (16). The required temperature measurements were obtained using Pt100 probes. Nitrogen (18) was fed in the two vessels to prevent oxidation in solution.

2.2 Fed-batch isothermal crystallization experiments

The crystallizer was initially filled with a saturated solution of hydroquinone, and kept at 25°C. During the first period of the semi-continuous operation (i.e. the first half an hour) a 'hot' solution was fed to the crystallizer. Afterwards, the suspension was kept at 25°C, under stirring, for about 1.5 hour, in order to let the slurry reach the equilibrium. Samples of the clear liquor in the crystallizer were withdrawn every 3 minutes. The solute concentration of these samples was determined through titration. The two dimensional crystal size distributions of final crystal samples were measured using image analysis.

3. EXPERIMENTAL RESULTS

3.1 Supersaturation profiles

The solute concentration data allowed the computation of the degree of supersaturation β, defined as the ratio of the solute concentration to the solubility.
A semi batch run (see Fig.3) consists of three phases. During phase 1, the solute concentration increases as the feeding solution presents a higher hydroquinone concentration. Phase 1 terminates when primary nucleation occurs. During phase 2 the solute concentration reaches a plateau: the feeding rate of hydroquinone is then constant and equal to the rate of consumption through particles growth. Phase 3 begins when the feeding rate falls to zero. A decrease of the solute concentration towards the solubility is then observed.
As expected, the presented experimental data also show that supersaturation tends to 0 at the end of phase 3.

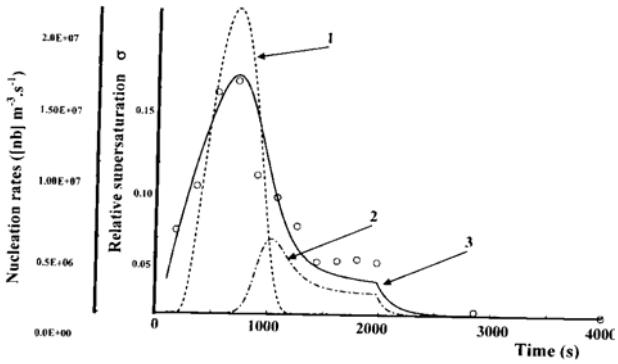

Fig. 3. Semi batch crystallization of hydroquinone Computed nucleation rates (dashed lines 1 and 2 for r_{N1} and r_{N2}); computed relative supersaturation σ (full line 3); measurements of the relative supersaturation σ (open circles)

3.2 Evolution of crystals sizes and elongation factor

To avoid undesirable thin needle crystal habits, a tailor-made additive was selected for its ability to reduce the growth along the length direction. The efficiency of such addition was clearly demonstrated

as the average length decreased with the additive concentration. The measured coefficients of variation are rather large: a unique period of crystals birth (i.e. through primary nucleation) is not consistent with such wide CSD. Consequently, secondary nucleation phenomena have to be considered for realistic further simulations.

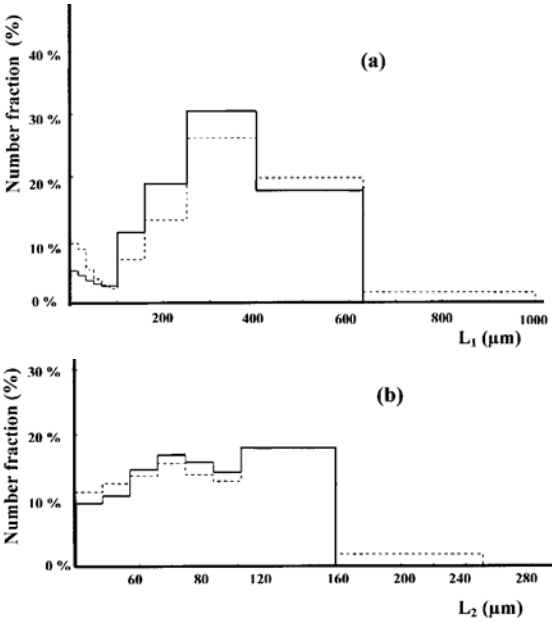

Fig. 4. Semi batch crystallization of hydroquinone (run SC2): Comparison between computed and measured number CSD of final crystals (a) Length L_1; (b) Width L_2. (Dashed lines: Measurements using Image Analysis; Full lines: Computed Final CSD)

Indeed, the size- and impurity-dependency of F_1 cannot be expressed by any simple and obvious relationship. For example, no satisfactory simulation of the variations of the crystal shape can be obtained assuming a constant elongation factor over the size range. Therefore, considering two dimensional population balances in the case of non-isotropic crystals presents a real interest for predictive modelling purposes. Obviously, the experimental data required for such modelling cannot be obtained through usual particle sizing techniques such as laser diffraction methods, as they only provide one equivalent size distribution. This is why image analysis was used (Fig.4)

4. ESTIMATION OF THE KINETIC PARAMETERS OF THE CRYSTALLIZATION

4.1 Kinetic modelling of the semi batch crystallization of hydroquinone

The main mechanisms encountered in the semi-batch crystallization of hydroquinone are primary and secondary nucleation, and growth. In the modelling breakage and agglomeration were assumed to be of second order of importance.

A detailed model describing the crystallization of hydroquinone, based on bi-dimensional population balance equations (PBE), was developed to compute the time variations of L_1 and L_2. The CSD was assumed not to depend on spatial coordinates in the well-mixed lab-scale crystallizer. The PBEs involve kinetics equations relating the mechanisms of crystallization mentioned above and mass balance equations. The whole model is presented in more details by Puel et al. (2003a). Table 1 summarizes the main equations which were considered in the case of well-mixed crystallizers.

A, B are primary nucleation coefficients that can be determined experimentally and have complex physical meaning (see e.g. Mersmann, 1996). k_N, *n, k* are parameters for the kinetic modelling of secondary nucleation. k_N is generally assumed to be related to the stirring power and to exhibit a temperature-dependency according to Arrhenius's law. Exponent *n* lies between 0.5 and 2.5. Exponent *k* is generally assumed to be of the order of 1 (Garside, 1985). $k_{i,1}$, $k_{i,2}$, j_1 and j_2 are growth parameters for the integration step of solute in the crystal lattice. $k_{i,1}$ and $k_{i,2}$ are the kinetic constants related to L_1 and L_2 directions, respectively, and j_1 and j_2 (in general 1 or 2) are the order of integration depending on the mechanism in question. k_d, is a mass transfer coefficient related to the diffusive step of solute in the layer around the crystal surface. η_1 and η_2 are effectiveness factors for faces 1 and 2 allowing to calculate the real mass flux density integrated in the crystal with respect to the maximal mass flux density that would be obtained in the absence of diffusive limitations (Garside, 1971).

Twelve parameters are thus involved, but the last three ones, which are time varying, can be calculated for every time step, using data available in the literature. Finally, nine kinetic parameters remain to be estimated from the experimental data through the fitting of the measured variables to the model-predicted ones.

4.2 Solving the bi-dimensional Population Balance Equations (PBE)

The method of classes was used for solving the bi-dimensional PBE, it requires the introduction of population number function $N(L_1,L_2,t)$. The crystals number function is discretized over the bi-dimensional size domain and $Ni,j(t)$ represents the number of crystals belonging to the class denoted by $Cl_{i,j}$. The program calculates the relative supersaturation σ, the kinetic rates of nucleation r_{N1} and r_{N2} and of growth G_1 and G_2 along the L_1 direction, respectively the L_2, axes. The total number and mass of crystals and the bi-dimensional size distribution are finally computed.

The spatial domain of crystals length and width (respectively L_1 and L_2) is first discretized and the smallest class of size is assumed to fit the characteristic nuclei represented by its two dimensions, L_1^* and L_2^*.

Let $L_{1,0}$,..$L_{1,i}$, ...$L_{1,im}$ be a suite of length where $L_{1,im}$ is the length of the largest crystals. These lengths define *im* classes quoted $Cl_{1,i}$, the extent of a class is $\Delta Cl_{1,i} = L_{1,i} - L_{1,i-1}$ and the characteristic length of the class is $S_{1,i} = (L_{1,i-1} + L_{1,i})/2$. The same discretization is performed for L_2.

As Fig.5 shows, such discretization defines bidimensional classes $Cl_{i,j}$, delimited by $L_{1,i}$, $L_{1,i-1}$, and $L_{2,j}$, $L_{2,j-1}$ of area $A_{i,j} = \Delta Cl_{1,i}\ \Delta Cl_{2,j}$. These classes are fixed and of constant size. The size domain is divided

in a system of *im* by *jm* bi-dimensional classes. The method of classes also requires the introduction of the population number function $N(L_1,L_2,t)$ defined as follows :

$$\frac{d^2N(L_1,L_2,t)}{dL_1 dL_2} = \psi(L_1,L_2,t) \quad (1)$$

The number of crystals belonging to the class $Cl_{i,j}$ can therefore be expressed as :

$$N_{i,j}(t) = \int_{L_{i-1}}^{L_i}\int_{L_{j-1}}^{L_j} \psi(L_1,L_2,t)dL_1dL_2 \quad (2)$$

im by *jm* number functions $N_{i,j}(t)$ are thus defined.

4.3 Application of the method of classes

To express the population balance equations, the population number function $N(L_1,L_2,t)$ are now used, rather than the population density function $\psi(L_1,L_2,t)$.

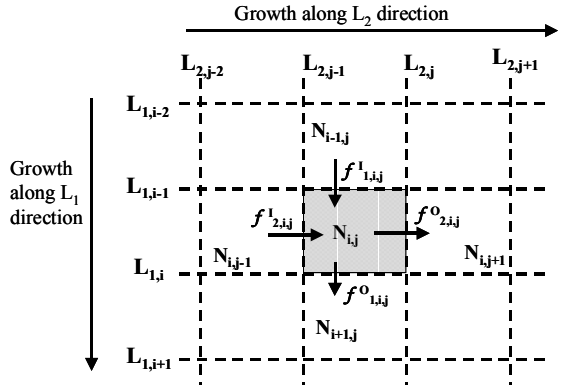

Fig. 5. Bi-dimensional class $Cl_{i,j}$, inlet flows of crystal numbers $f^{I}_{1,i,j}$; $f^{I}_{2,i,j}$ and outlet flows of crystal numbers $f^{O}_{1,i,j}$; $f^{O}_{2,i,j,}(t)$

1. The balance equation (T1) (see Table 1) is first discretized according to the bi-dimensional grid presented above (see also Fig.5):
The PBE is integrated after combining expressions (2) and (T1) with :

$$\int_0^\infty\int_0^\infty R_N dL_1 dL_2 = r_{N1} + r_{N2} \quad (3)$$

2. The population balance around the bi-dimensional class $Cl_{i,j}$ leads to a set of *im* by *jm* ordinary differential equations :

$$\frac{1}{V_T(t)}\frac{d}{dt}\left[N_{i,j}(t)V_T(t)\right] + f_{1,i,j}(t) + f_{2,i,j}(t) + \quad (4)$$

$$+\frac{F(t)N(L_1,L_2,t) - F_{in}(t)N_{in}(L_1,L_2,t)}{V_T(t)} = r_{N1} + r_{N2}$$

$f_{1,i,j}(t)$ and $f_{2,i,j}(t)$ are the net inlet and outlet flows of crystals in class $Cl_{i,j}$, in the length and width directions induced by growth, respectively. Each crystals flow being divided in inlet and outlet flows for each direction (see arrows on Fig.5)

$$f_{1,i,j,}(t) = f^{O}_{1,i,j,}(t) - f^{I}_{1,i,j,}(t) \quad \text{and}$$
$$f_{2,i,j,}(t) = f^{O}_{2,i,j,}(t) - f^{I}_{2,i,j,}(t) \quad (5)$$

Where $f^{O}_{1,i,j}(t)$, $f^{O}_{2,i,j}(t)$ are the outlet crystal flows from the $Cl_{i,j}$ class in the L_1 and L_2 directions ; and $f^{I}_{1,i,j}(t)$, $f^{I}_{2,i,j}(t)$ are the inlet crystal flows from the $Cl_{i,j}$ class in the L_1 and L_2 directions

The calculation of these inlet and outlet crystal fluxes are carried out using a first-order Tailor series expansion:

$$f^{O}_{1,i,j}(t) = G_1(S_{1,i},t)\left[a_{1,i}N_{i,j}(t) + b_{1,i}N_{i+1,j}(t)\right] \quad (6)$$

$$f^{I}_{1,i,j}(t) = G_1(S_{1,i-1},t)\left[a_{1,i-1}N_{i-1,j}(t) + b_{1,i-1}N_{i,j}(t)\right]$$

with $$a_{1,i} = \frac{\Delta Cl_{1,i+1}}{\Delta Cl_{1,i}(\Delta Cl_{1,i+1} + \Delta Cl_{1,i})} \quad (7)$$

$$b_{1,i} = \frac{\Delta Cl_{1,i}}{\Delta Cl_{1,i+1}(\Delta Cl_{1,i+1} + \Delta Cl_{1,i})} \quad (19)$$

and $$f^{O}_{2,i,j}(t) = G_2(S_{2,j},t)\left[a_{2,j}N_{i,j}(t) + b_{2,j}N_{i,j+1}(t)\right] \quad (8)$$

$$f^{I}_{2,i,j}(t) = G_2(S_{2,j-1},t)\left[c_{j-1}N_{i,j-1}(t) + d_{j-1}N_{i,j}(t)\right]$$

with $$a_{2,j} = \frac{\Delta Cl_{2,j+1}}{\Delta Cl_{2,j}(\Delta Cl_{2,j+1} + \Delta Cl_{2,j})} \quad (9)$$

$$b_{2,j} = \frac{\Delta Cl_{2,j}}{\Delta Cl_{2,j+1}(\Delta Cl_{2,j+1} + \Delta Cl_{2,j})}$$

The previous expressions are valid for $2<i<im-1$ and $2<j<jm-1$. Only four neighbouring classes of $Cl_{i,j}$ are considered in the design of the algorithm. Particular cases are considered for the classes which are set at the boundaries of the size domain. The lower classes can not accept growing crystals form the previous ones: $f^{I}_{1,1,j}(t) = f^{I}_{2,i,1}(t) = 0$. Crystals in the upper classes can not grow in the next ones: $f^{O}_{1,im,j}(t) = f^{O}_{2,i,jm}(t) = 0$. Other numerical treatments are necessary and are reported by Puel (1994).

4.4 Parameter estimation and simulation results

Data were collected after six experiments which correspond to four concentrations of tailor-made additive (i.e. 0, 400, 600 and 1000 ppm).
'Usual' optimisation procedures would obviously lead to an excessive computational time and are likely to converge towards local optima. The applied estimation strategy was therefore based on the use of mechanistic knowledge of the crystallization system to save time and to make the convergence easier. Such strategy was successfully applied by David et al. (1991), it is based on the fact that different mechanisms occur successively during this semi batch crystallization process: as outlined above there are 3 main periods during which each mechanism prevails even though until the end of the process, secondary nucleation should be considered as a potential mechanism for the generation of nuclei. In practice the estimation procedure is therefore driven as follows:
Firstly, the exponents involved in the growth kinetic are arbitrarily fixed at $j_1=j_2=1$. The CSD is computed and the calculated and measured mono-dimensional crystals distributions are compared, successively in the L_1 and L_2 directions. To stress on the bi-dimensional information, the simulated and experimental elongation factor F_1 are also compared. By this way, a precise choice of the kinetic orders n, k , j_1 and j_2 can be performed. The values of A, B, k_N, $k_{i,1}$ and $k_{i,2}$ are then tuned using a trial and error approach based on the physical meaning of the parameters which have to be estimated. More details

on the parameter estimation are reported by Puel et al. (2003b).

Run SC4. Run SC4, carried out with 600 ppm of additive, was first selected. Fig. 3 presents the measured and calculated relative supersaturation. The model prediction is good until the supersaturation reaches the plateau, where the simulation underestimates the steady-state supersaturation. The obtained value of B is rather low, leading to a large burst of primary nucleation peak during few minutes. Actually, A and B are strongly linked together through the total number of crystals, a reduction of B leads to an increase of A. Nevertheless, the maximum estimated supersaturation value, which corresponds to the limit of the metastable zone, is correctly predicted. The kinetic coefficients and orders of secondary nucleation were then fitted to represent the population of fine crystals in the final CSD (see Fig. 4)). Again, the four kinetic parameters related to the two growth laws are strongly connected. Values 1 and 2 for the orders j_1 and j_2 lead to 4 possible combinations. Setting $j_1=j_2=2$ or $j_1=j_2=1$ leads to underestimate, respectively overestimate, the decrease of supersaturation after primary nucleation. Additional information was then obtained from the measurements of the elongation factor F_1, which is very sensitive to differences in the growth rates along the two main directions. Finally, setting $j_1=2$ and $j_2=1$ allowed the best prediction of the particle shape. Any other value of j_1 and j_2 leading to a maximum for F_1, which was not experimentally observed. The growth coefficients $k_{i,1}$ and $k_{i,2}$ were finally set considering the main population of crystals in the final distribution (see Fig. 4). For the experiment in question, the length and width of crystals were satisfactorily predicted.

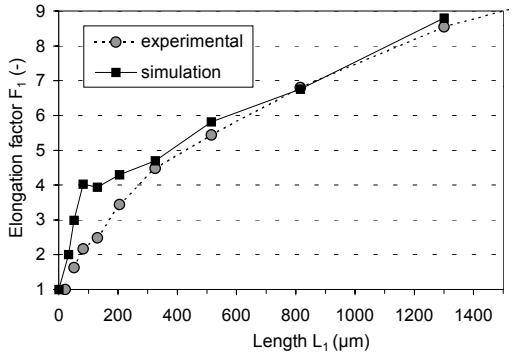

Fig. 6. Semi-batch crystallization of hydroquinone (run SC1). Experimental and model-predicted evolution of the elongation shape factor F_1 vs. L_1 (Average of a sample of final crystals)

Runs SC1, SC2 and SC5. Some of the kinetic parameters estimated after run SC4 should be modified in order to account for the effect of the concentration of additive.

The orders of the growth and secondary nucleation kinetic laws (n, k, j_1 , j_2) were unchanged since no modification of the two mechanisms involved was expected from the introduction of additive. Due to the chemical structure of the additive, it was also assumed that the growth in the L_2 direction was not altered so that $k_{i,2}$ was kept constant. Moreover the experiments showed that primary nucleation was increasingly delayed by increasing amounts of additive. Parameters A and B being linked each other, A was assumed constant and then B fitted in order to represent the measured maximal supersaturation in the neighbourhood of primary nucleation. The level of fine particles in the CSD and the final total number of crystals is dependent on the primary and secondary nucleations. The prediction of the number of crystals was achieved through the evaluation of appropriate values of the kinetic coefficients B and k_N related to the law for nucleations. Moreover, in order to reproduce the reduction of the experimental elongation factor with increasing concentrations of additive – which, indeed, is the effect expected from the use of the selected additive – it was necessary to assess a decreasing relationship between the value of $k_{i,1}$ and the concentration of additive.

The three parameters mentioned above (i.e. B, k_N and $k_{i,1}$) were first estimated for runs SC2 (400 ppm of additive) and SC5 (1000 ppm of additive) by comparing experimental and simulation results. The fit obtained between experimental and simulated data was correct. Unfortunately, for run SC1 (0 ppm of additive), no supersaturation measurement was available. Consequently, in order to extend the set of kinetic parameter values, the missing parameters of B, k_N *and* $k_{i,1}$ were extrapolated at 0 ppm. Second order polynomial and linear relationships between the three kinetic parameters and the concentration of additives were established As one can see in Fig. 6, the simulated elongation factor for run SC1 obtained with the extrapolated parameters at 0 ppm was in good agreement with the experimental data, the model and the set of kinetics parameters were therefore considered as validated.

5. GENERAL REMARKS AND DISCUSSION OF THE RESULTS

As far as the estimation of numerous kinetic parameters is involved, it is our opinion that, given the limited number of experimental data and the complexity of the crystallization phenomena, the use of an optimization algorithm would lead to uncertain parameters and finally to a poor predictive ability of the model. Putting physical knowledge in the modeling allowed more efficient and more reliable convergence towards a satisfactory representation of the semi-batch crystallization operations.

The main originality of the present work lies in its two-dimensional approach for the modeling of particle shape, and almost no such application based on real experimental data can be found in the literature. This work is also an attempt to relate the effect of a specific tailor-made additive to the shape of hydroquinone crystal.

Primary nucleation appears to be quite sensitive to the concentration of additive as the delay of nuclei formation increases with the additive concentration. The molecules of additive turn out to act as nucleation inhibitors, maybe by limiting the growth of crystal embryos. The concentration dependency of parameter B estimated during the present work relates the increase of the width of metastable zone associated to such inhibition effect. Secondary

nucleation was taken into account to explain the fractions of fine crystals in the final experimental CSD, even though this is not the major mechanism for nuclei generation.

A major impact of the additive on the crystal habit was also observed and simulated. The molecules of additive act as efficient growth inhibitors in the length direction so that between 0 and 1000 ppm, the growth rate kinetic coefficient $k_{i,1}$ is divided by a factor of 3.2. Again, this result is consistent with physical considerations.

6. CONCLUSIONS

A bi-dimensional population balance approach was developed for simulating the time variations of the habit of non isotropic crystals of hydroquinone during solution crystallizations. The algorithm coupled with kinetic models allowed the simulation of isothermal semi-batch crystallization of hydroquinone exhibiting a rod-like habit. Despite various experimental conditions, the supersaturation profiles were correctly predicted, and the computed final bi-dimensional CSD and elongation shape factors fit the experimental data.

An inhibition effect of a tailor made additive was clearly observed, and represented by the model. The additive mainly affects primary nucleation and the growth in the length direction, but secondary nucleation mechanisms and their inhibition in the presence of additive were also taken into account and successfully represented, allowing a good prediction of the final content of the slurry in fines particles.

A set of nine kinetics parameters was estimated through the comparison between experimental and calculated data.

The reported parameter values were partly validated trough the prediction of a semi-batch crystallization performed without additive. Three kinetic parameters were related to the concentration of additive in order to represent the inhibition effects of the tailor-made additive but, even though their physical consistency was justified, the obtained relationships are simply phenomenological.

REFERENCES

David R., J., Villermaux, P., Marchal, J.P. Klein (1991).Crystallization and precipitation engineering – IV. Kinetic model of adipic acid crystallization. *Chem. Eng. Sci.*, **46**,4,1129-1136.

Franck R., R., David, J., Villermaux, J.P., Klein (1988). Crystallization and precipitation engineering. II. A chemical reaction engineering approach to salicylic acid precipitation. *Chem. Eng. Sci.*, **43**,1,69-77

Garside, J. (1971). The concept of effectiveness factors in crystal growth. *Chem. Eng. Sci.*, **26**, 1425-1431.

Garside, J. (1985). Industrial crystallization from solution. *Chem. Eng. Sci.*, **40**,1,3-26.

Mersmann, A., (1996). Supersaturation and nucleation. *Trans.IChem E.,* **74**, Part A, 812-820.

Puel, F. (1994). Bilan de population pour deux tailles caractéristiques de particules : application à la crystallisation de l'hydroquinone. Ph-D Thesis Université Lyon 1, (in French)

Puel F., G., Fevotte, J.P., Klein. (2003a). Simulation and analysis of industrial crystallization processes through multidimensional population balance equations. Part 1: A resolution algorithm based on the method of classes. To appear in *Chem. Eng. Sci*

Puel F., G., Fevotte, J.P., Klein. (2003b). Simulation and analysis of industrial crystallization processes through multidimensional population balance equations. Part 2: A study of semi batch crystallization. To appear in *Chem. Eng. Sci.*,

Table 1. Main equations of the crystallization model in the case of well-mixed crystallizers

Population balance for two main sizes (L_1 and L_2)	$\frac{1}{V_T(t)}\frac{\partial}{\partial t}\left[\psi(L_1,L_2,t)V_T(t)\right]+\frac{\partial}{\partial L_1}\left[G_1(L_1,t)\psi(L_1,L_2,t)\right]+\frac{\partial}{\partial L_2}\left[G_2(L_2,t)\psi(L_1,L_2,t)\right]$ $+\frac{F(t)\psi(L_1,L_2,t)-F_{in}(t)\psi_{in}(L_1,L_2,t)}{V_T(t)}=R_N(L_1,L_2,t)$	(T1)
	with $\int_0^{\infty}\int_0^{\infty} R_N\,dL_1dL_2=\int_0^{L_1^*}\int_0^{L_2^*} R_N\,dL_1dL_2=r_{N1}+r_{N2}$	(T2)
Primary nucleation	$r_{N1}=A.\exp\left(-\frac{B}{\ln^2\beta}\right)$	(T3)
Secondary nucleation	$r_{N2}=k_N.\sigma^n M_T^k$	(T4)
Growth L_1 direction	$G_1(t)=2\frac{M_s}{\rho_s}\eta_1.k_{i,1}(C(t)-C^*(T(t))^{j_1}$ with	(T5)
	$\left[\frac{k_{i,1}}{k_d}[C(t)-C^*(T(t))]^{j_1-1}\right]\eta_1+\eta_1^{1/j_1}-1=0$	
Growth L_2 direction	$G_2(t)=2\frac{M_s}{\rho_s}\eta_2.k_{i,2}(C(t)-C^*(T(t))^{j_2}$ with	(T6)
	$\left[\frac{k_{i,2}}{k_d}[C(t)-C^*(T(t))]^{j_2-1}\right]\eta_2+\eta_2^{1/j_2}-1=0$	
Mass balance	$f_{in}(t)C_{in}(t)=F_{in}(t)C_{in}(t)=\frac{d\left[V(t)C(t)+V_T(t)C_s(t)\right]}{dt}$	(T7)